JOURNAL OF GEOPHYSICAL RESEARCH, VOL. 99, NO. A6, PAGES 11,319–11,326, JUNE 1, 1994

A large magnetosphere magnetic field database

D. H. Fairfield and N. A. Tsyganenko

Laboratory for Extraterrestrial Physics, NASA Goddard Space Flight Center, Greenbelt, Maryland

A. V. Usmanov

Institute of Physics, University of St. Petersburg, St. Petersburg, Russia

M. V. Malkov

Institute of Informatics and Mathematical Modeling, Apatity, Russia

Abstract. A large magnetosphere magnetic field database compiled from the measurements of 11 Earth-orbiting spacecraft during 1966–1986 is described. The 11 contributing spacecraft (Explorer 33 and 35, IMP 4, 5, 6, 7 and 8, Heos 1 and 2, and ISEE 1 and 2) provide data between $4R_E$ and $60R_E$, which have been edited in order to exclude data outside the magnetosphere. Currently, the database totals more than 79,000 records, which sum to a total of more than 1600 spacecraft days in the magnetosphere. Each of these records contains the average total field vector in geocentric solar magnetospheric coordinates, disturbance field vector (measured field minus Earth's internal field), time information, spacecraft position, AE, AL, Kp, and Dst geomagnetic indices, and associated solar wind and interplanetary magnetic field parameters when available. These data have constituted and will undoubtedly continue to constitute the standard database for magnetospheric modeling studies. They are also appropriate for statistical studies of the magnetic field and its dependence on solar wind quantities. Plans are to update this database in the future with data from additional spacecraft.

Introduction

Knowledge of the Earth's magnetic field is of critical importance in the study of magnetospheric physics. The magnetic field influences the motions of electrons and ions whose differing motions are responsible for the electric currents that in turn perturb the magnetic field. Over the past 30 years numerous spacecraft, sometimes making more than 10 vector measurements per second for year after year, have made hundreds of millions of vector measurements throughout the magnetosphere. These measurements were made at many different locations and for a variety of solar wind conditions, but at these high sampling rates the resolution both in space and time is much finer than what is needed in many applications. To reduce this immense quantity of data to a manageable size, it is necessary to create averages so that consecutive values correspond to significantly different locations and to solar wind/magnetospheric conditions that may be different. In this report we describe a large magnetosphere magnetic field database that has been constructed from the measurements of 11 different spacecraft over an interval of 20 years. Parts of this database have already been used in the construction of average magnetosphere models [*Mead and Fairfield*, 1975; *Tsyganenko and Usmanov*, 1982; *Tsyganenko*, 1987, 1989; *Peredo et al.*, 1993]. The database will continue to be updated and will undoubtedly serve for this and other purposes for years to come.

Paper number 94JA00255.
0148-0227/94/94JA-00255$05.00

History of the Database

Construction of the large magnetospheric database began in the early 1970s when *Mead and Fairfield* [1975] embarked on a project to produce the first quantitative magnetosphere magnetic field model derived from actual spacecraft measurements. Their modeling techniques were most appropriate in the near-Earth region so they limited their data compilation to that within $17R_E$. They utilized data from four eccentric Earth-orbiting spacecraft and choose $0.5R_E$ as a reasonable averaging interval for their radially moving spacecraft; such intervals are typically 10 to 25 min long, depending on radial distance and the exact orbit. That choice of the averaging time intervals (ΔT)/orbit segments (ΔS) can be justified by noting that the corresponding characteristic scales ΔT and ΔS are commensurate with the best temporal/spatial resolution that is "marginally available" from average global models. More quantitatively, in the near magnetosphere ($4R_E < R < 10R_E$) the smallest characteristic scale length for such persistent features as the ring current and the tail current sheet is of the order of $1R_E$, while the characteristic timescale for buildup and decay of the principal current systems (leaving aside rapid substorm-related phenomena) are unlikely to be less than 10–20 min. Such times are also commensurate with typical travel times of the Alfven waves within the same region.

When *Tsyganenko and Usmanov* [1982] started developing models in the early 1980s they extended the techniques of *Mead and Fairfield* [1975] and included models of the magnetotail and ring current. The data base they used was that of *Mead and Fairfield* [1975] augmented by the HEOS 1 and 2 data taken during 1969–1974 which covered the high-latitude magnetosphere in the northern hemisphere [*Hedgecock*, 1975; *Hedgecock and Thomas*, 1975]. In later efforts [*Tsyganenko*, 1987, 1989] the modeled region was extended tailward, and that required including data taken in the magnetotail by IMP spacecraft. The tail data were obtained from the National Space Science Data Center (NSSDC) in the form of hourly averages for $X < -15R_E$ and $(Y^2 + Z^2)^{1/2} < 30R_E$. The last requirement was imposed in order to crudely eliminate measurements taken outside the magnetosphere; a more accurate selection was carried out when creating the final data set, based on an empirical analytical model for the average magnetopause shape [*Tsyganenko*, 1976, 1981]. Actually, the magnetopause is a very dynamic boundary, and therefore tail data should be selected for individual orbits after viewing high-resolution data plots. However, because of lack of plotting facilities in Russia at that time, it was only possible to use the formal selection method with a single analytical model of the magnetopause. This method undoubtedly led to omission of some magnetospheric data near the tail boundary and, conversely, to erroneous inclusion of magnetosheath measurements taken during strong compressions and/or transient deflections of the tail during periods with significant nonradial flow of the solar wind. Also, intervals of bad data produced by telemetry noise or other anomalies were undoubtedly included.

Subsequently, Tsyganenko and Malkov [see *Peredo et al.*, 1993] added ISEE 1/2 data to the database, while Fairfield independently added HEOS data along with additional IMP 6 data to the original Mead-Fairfield database. Below we describe the additional editing of these data sets and their merging into one large magnetosphere database. Characteristics of the various contributing spacecraft are as follows.

Contributing Spacecraft

The Explorer 33 spacecraft was launched in July 1966 with the objective of entering lunar orbit. Explorer 33 failed to achieve lunar orbit but provided data from a highly eccentric Earth orbit with apogee near $80R_E$. The magnetometer experiment [*Ness et al.*, 1967a] was a triaxial fluxgate magnetometer, as were all instruments contributing to the database described here. The spacecraft spun with an average spin period near 2.4 s about an axis oriented near the ecliptic plane and provided a vector field sample every 5.1 s. Only Explorer 33 data within $17R_E$ is included here.

Explorer 35 was launched into a lunar orbit in July 1967 and hence provided distant tail measurements for 2 to 3 days every month as the moon passed through the magnetotail. The spacecraft spun with a period of 2.3 s about an axis oriented perpendicular to the plane of the ecliptic. The spacecraft automatically switched between ranges of ±24 and ±64 nT and magnetic field vectors were sampled every 5.1 s [*Ness et al.*, 1967b]. The Explorer 35 spacecraft flipper, used to invert the sensors and help correct instrument zero levels, failed after almost 2 years of operation making the subsequent zeros somewhat less certain. Although the spacecraft produced data for some 5 years, only data from the initial 2 years are included here.

The IMP 4 spacecraft was launched in May 1967 into an eccentric orbit with an inclination of 67.4° and an apogee of $31.4R_E$ near the ecliptic plane. IMP 4 was a spinning spacecraft with an initial spin rate of 2.587 s and an orbital period of 4.32 days [*Fairfield*, 1969]. The magnetometer provided a vector measurement every 2.556 s and had ±32 and ±128 nT sensitivity ranges that were controlled by ground commands. The low-sensitivity range allowed measurements to be made as close to the Earth as approximately $6.5R_E$. Occasions when unusually strong fields saturated the instrument in the low range were edited out of the data set. The instruments were mounted on 6-foot (1.8 m) booms, and the spacecraft was magnetically clean so zero levels are thought to be accurate to better than 0.3 nT. The magnetometer experiment provided vector measurements from launch until a solar sensor failure in March 1969 that occurred just 2 months prior to spacecraft reentry to the atmosphere.

The IMP 5 spacecraft was launched in June 1969 into an eccentric orbit with inclination 86.8° and an apogee of $28.7R_E$ [*Fairfield and Ness*, 1972]. Although its apogee was near the ecliptic plane, IMP 5 was near the noon meridian at the time of maximum dipole tilt which allowed measurements of the polar cusp at geomagnetic latitudes as high as 75° beyond $6R_E$. The experiment was almost identical to IMP 4 except that the ranges of ±40 and ±200 nT allowed measurements as close to the Earth as $5.5R_E$. The IMP 5 magnetometer provided 381 orbits of data prior to spacecraft reentry in December 1972.

The IMP 6 spacecraft was launched in March 1971 into an eccentric orbit with inclination 28.7° and an apogee of $33.1R_E$. IMP 6 underwent one spin every 11.1 s and the orbital period was 4.18 days [*Fairfield*, 1974]. The experiment provided data at a rate of 12.5 vector measurements/s. Instrument ranges of ±16, ±48, ±144, and ±432 nT were changed automatically depending on the measured field, thus allowing measurements as close to the Earth as $4R_E$ without data losses due to the instrument being in an inappropriate range. The sensors were located on the end of a 13-foot (4 m) boom and a spacecraft contamination field was no problem. Zero levels are thought to be accurate to ±0.3 nT in the least sensitive range and better in more sensitive ranges. IMP 6 provided over 300 orbits of data until spacecraft reentry in October 1974.

The IMP 7 and 8 spacecraft carried identical instruments (R. P. Lepping et al., IMP-8 solar wind magnetic field and plasma data in support of Ulysses-Jupiter encounter: January 13–31, 1992, Appendix A, internal document, NASA Goddard Space Flight Center, Greenbelt, MD., 1992). IMP 7 was launched in September 1972 and provided data until an instrument failure in April 1973. IMP 8 was launched in October 1973, and the magnetometer continues to provide data at the time of this writing 20 years later. Both spacecraft had roughly circular orbits near $35R_E$; actual apogee and perigee distances varied but were generally near $40R_E$ and $30R_E$ respectively. The orbital period of both spacecraft was roughly 12 days. The spacecraft usually resided in the magnetotail for 2 to 3 days each orbit, but during some seasons IMP 8 passed north or south of the tail and provided little magnetotail data.

The HEOS 1 and 2 spacecraft were launched on December 5, 1968, and January 31, 1972, respectively, into orbits with initial apogees of $35.8R_E$ and $38.7R_E$ respectively [*Hedgecock*, 1975]. The initial ecliptic latitudes of the two apogee were 51.5° and 73.5°, and both increased by more than 10 deg thus providing unique coverage of the polar magnetosphere not available from the IMP spacecraft. HEOS 1 and 2 each carried a single range instrument with ranges ±64 and ±144 nT, respectively, that provided measured vectors every 48 and 32 s respectively. HEOS 2 reentered the Earth's atmosphere in August 1974; HEOS 1 continued to operate but tracking diminished.

The ISEE 1 and 2 spacecraft [e.g., *Ogilvie et al.*, 1978; *Russell*, 1978] were launched in October 1977 into almost coincident eccentric orbits with apogee of nearly $23R_E$, orbital periods of about 2.4 days, and orbit inclination of 29°. The spacecraft were placed in a spinning mode with 3 s spin period and the spin axis aligned nearly perpendicular to the solar ecliptic plane. The spacecraft provided data until their reentry in September 1987. For now, we include data only for the first four years of the experiment, from the beginning of 1978 to the end of 1981. The magnetometer experiments onboard both ISEE spacecraft [*Russell*, 1978] were triaxial fluxgate instruments having two commandable ranges, ±8192 and ±256 nT. Our data set is constructed from 1-min average tapes from ISEE 2 (January 1978 to January 1980) and ISEE 1 (January 1980 to December 1981) obtained from NSSDC. Because of fixed orientation of the ISEE orbits in inertial space, the spacecraft provided magnetotail data between February and May, while the dayside magnetosphere was swept mainly from August to November.

Data Description

The current data set that we describe in this paper is basically the $R < 17R_E$ IMP half-Earth-radii averages within $17R_E$ of the Earth and the IMP hourly averages beyond $X = -15R_E$, which are augmented by HEOS and ISEE averages computed in a slightly different manner (see below). We now describe how the database was constructed.

The initial compilation of the large magnetosphere database utilized data from four eccentric Earth-orbiting spacecraft (IMP 4, 5, and 6 and Explorer 33) [*Mead and Fairfield*, 1975]. Data that had already been averaged to resolutions ranging from 15 to 81 s were used as the initial data. These data were plotted for individual inbound and outbound orbital passes and at the same time averages of the magnetic field were calculated over half-Earth radii intervals separated by half-integral values of the geocentric distance in units of Earth radii. Associated ephemeris elements were averaged in the same manner. Although the inclination and declination values were also averaged at this time and were available in an early version of this data set, these quantities have been omitted from the present data set and only Cartesian component averages have been retained. The Earth's internal (IGRF) field was also subtracted from the measurements and both the total field vector and the difference field are retained. The duration of the averaging periods depend on spacecraft orbit and position in the orbit, but they generally range from 10 to 25 min. Since modeling the inner magnetosphere was the goal at that time, this data set was restricted to distances less than $17R_E$. Additional IMP 6 data totaling more than 6800 average points was later processed in the same manner and added to the original compilation. In the $R < 17$ data the average of individually measured field magnitudes (as opposed to the square root of the sum of the square of component averages) is not available as it is in most of the remainder of the data set.

IMP data beyond $X_{\rm GSM} = -15R_E$ consist of hourly average measurements from the magnetic field experiments of N. F. Ness on the spacecraft Explorer 33 and IMP 4, 5, 6, 7, and 8. Data within $30R_E$ of the Earth-Sun line and $X < -15R_E$ were initially considered and then hours containing any magnetosheath data or data contaminated by telemetry noise were rejected based on visual scanning of data plots of individual orbits. Such plots were generally of points at 15- or 20-s resolution. Distinguishing the stronger quiet fields of the tail lobe from fluctuating fields of the magnetosheath is relatively straightforward. Distinguishing plasma sheet from magnetosheath is more difficult but with the use of a high-resolution standard deviation that helps identify the presence of magnetosheath waves, a decision is often possible. For the IMP 6, 7, and 8 data, plots of the plasma data from the Los Alamos National Laboratory plasma experiments were usually available to help distinguish the regions in ambiguous cases. Erroneous decisions are more likely for IMP 4 and 5 and Explorer 35, but attempts were made to reject ambiguous data in order to insure a clean magnetotail data set. In addition, it was required that at least 15 min worth of the hours data be present before an hourly average was retained. After the IMP 8 data had been processed and edited it was discovered that during occasional intervals during 1981–1986 the IMP 8 spin axis orientation was in error by as much as a few degrees (R. P. Lepping, private communication, 1993). These intervals were removed from the data set reducing the available IMP 8 data by something like 15%.

HEOS data currently consists of spatially averaged data at $0.5R_E$ resolution that the principal investigator provided to one of us (N.A.T.) in the form of listing and that were subsequently transcribed to digital form. Although these data have similar resolution to the IMP data, they were averaged in a somewhat different manner. The solar magnetospheric coordinate system was divided into $1R_E$ cubes and averages were constructed within various cubes as the spacecraft moved through GSM space on each orbit. Successive averages generally had radial distance differences between a few tenths of an Earth radius and $1R_E$. Times and average positions were provided with the data, but the times were center points of the averaging interval and durations of the averages were not available. For this reason it was impossible to calculate average AE/AL indices over the original averaging intervals. To overcome this difficulty, it was assumed the data were continuous and averages were calculated for times determined from the times between successive points. Since gaps in the data could lead to unrealistically long intervals, an upper limit of 35 min was placed on the AE/AL averaging time. As is the case with the IMP $< 17R_E$ data, the average of individually measured field magnitudes is not available in this data set. We plan to eventually reconstruct the HEOS database to make it more consistent with the other data.

ISEE data have also been processed slightly differently from the IMP data. First, a crude selection was accomplished by eliminating measurements taken well outside the magnetosphere and the magnetosheath, as well as those made too close to the Earth (closer than $4R_E$). Then plots of the **B** components were inspected in order to locate the magnetopause crossings and allow a finer selection of the data within the magnetosphere. No plasma data was used for identifying transitions between the magnetosphere and magnetosheath regimes, but available simultaneous measurements of solar wind plasma and the interplanetary magnetic field were used along with the **B** plots to aid in this determi-

Table 1. Available Data

Spacecraft	Time Interval Used	No Points With $X > -15R_E$	No Points With $X < -15R_E$	Total Time, hours	Number Orbits	Instrument Range, maximum
A-IMP D (Explorer 33)	July 1966 to July 1968	719	5	356	34	+64
A-IMP E (Explorer 35)	July 1967 to Jan. 1969	0	1260	1260	17	+64
IMP 4 (IMP F, Explorer 34)	May 1967 to Sept. 1971	3390	1783	2799	144	+128
IMP 5 (IMP G, Explorer 41)	June 1969 to Sept. 1971	5490	3936	5480	195	+200
IMP 6 (IMP I, Explorer 43)	March 1971 to Sept. 1974	9509	2292	5419	312	+432
HEOS 1	Dec. 1968 to Dec. 1973	3423	485	1980	215	+64
HEOS 2	Feb. 1972 to Aug. 1974	3044	0	1320	152	+144
IMP 7, (IMP H, Explorer 47)	Sept. 1972 to April 1973	0	681	650	14	+36
IMP 8, (IMP J, Explorer 50)	Oct. 1973 to June 1986	0	9568	8052	280	+36
ISEE 1	Jan. 1980 to Dec. 1981	13,613	3989	6794	301	+8192
ISEE 2	Jan. 1978 to Jan. 1980	12,628	3930	6497	311	+8192
Totals		51,816	27,929	40,607		

nation. Intervals of bad data were also identified and excluded based upon the visual checking of the magnetic field plots. The Earth's internal field was then subtracted from the 1-min **B** averages, using the 10-order IGRF expansions and taking into account the secular changes by an appropriate updating of its coefficients to given year of measurement. Then the 1-min external field components, the total vector components and the spacecraft position were all averaged along individual orbit segments; lengths of the segments were restricted not to exceed $0.5R_E$ in distance and 30 min in time. (The latter limitation comes into effect near apogee where the spacecraft speed becomes quite small.) An additional requirement was that the total number of individual 1-min values contributing to each average be no less than six.

During the course of this study, comparisons of simultaneous IMP 8 and ISEE data when both spacecraft were in the solar wind revealed times when the ISEE spin axis (B_z) field component was in error by nearly 2 nT. Although this apparently is not a common occurrence, the ISEE principal investigator is currently rechecking and validating this data. Should it prove necessary, the ISEE data in our data set will be rerun should improved data become available.

Hourly average solar wind and interplanetary magnetic field (IMF) data compiled by J. H. King at the NSSDC [*King*, 1977] have been associated with each magnetosphere field average when available. If the ISEE interval spanned consecutive hours, a linear interpolation of the interplanetary data was made for the 2 hours. If one of the two hours was missing the available hour was used. For other spacecraft the hourly average associated with the middle of the averaging interval was the value selected. *Dst* and *Kp* geomagnetic indices from the King data set were also included. Although most quantities are well known and are further described below, users should note that the solar wind longitude angles are given in a coordinate system in which the measured Y component of velocity introduced by the Earth's (and measuring spacecraft's) motion around the Sun has been removed. Magnetosphere researchers who want to know the solar wind direction "seen" by the magnetosphere should reintroduce this velocity-dependent component.

The 2.5- or 1-min geomagnetic *AE* and *AL* indices were also averaged over the same intervals as the individual field averages and inserted into the data set. These *AE*/*AL* data had been produced at NSSDC for the early years, the U.S. National Geophysical and Solar-Terrestrial Data Center for subsequent years, and World Data Center C2 for Geomagnetism at Kyoto University in Japan since 1978. Since *AE* data for 1976 and 1977 has never been produced, these years were omitted from the data set so that every record in the data set could have an associated *AE* value. IMP 8 data more recent than 1986 have also not been included due to the lack of *AE* at the time of production.

Table 1 lists the amount of available data by spacecraft. Column 1 lists the spacecraft and column 2 the interval of data used. Column 3 indicates the number of magnetosphere data points with $X_{\mathrm{GSM}} > -15R_E$ and column 4 gives the number of magnetotail averages ($X_{\mathrm{GSM}} < -15R_E$). Total time of the data from each spacecraft is listed in column 5. The number of orbits available for each spacecraft (estimated approximately in some cases) is listed in column 6; for the spacecraft with perigees at low altitudes, this number is roughly half the number of radial passes, which is roughly the number of independent data points in each half-Earth-radii interval. The most insensitive range of the instrument, as an indicator of the maximum field strength measured, is shown in column 7. Note that the possible errors of a few tenths of a nanotesla in the spin axis zero levels are thought to be the primary source of instrumental errors in weak fields. These are invariably much smaller than both day-to-day variations and ambient field variations over the averaging period. Fraction-of-a-degree errors in spacecraft orientation are the major source of error at low altitudes and are the reason for omitting ISEE 1/2 data at these distances.

Data Distribution

The data in this database are given in a right-handed orthogonal geocentric solar magnetospheric (GSM) coordinate system where the X axis is the Earth-Sun line and the Z axis is in the plane of the Earth's dipole and the X axis. In some case we will refer to solar magnetic (SM) coordinates where the Z axis is aligned with the dipole and the X axis is in the plane of the Earth-Sun line and the Z axis.

Figures 1a–1c illustrate the distribution of data. Figure 1a shows all data, except ISEE, for $X_{\mathrm{GSM}} > -15R_E$ with the distance $YZ = (Y_{\mathrm{SM}}^2 + Z_{\mathrm{SM}}^2)^{1/2}$ plotted versus X_{SM}. The sign

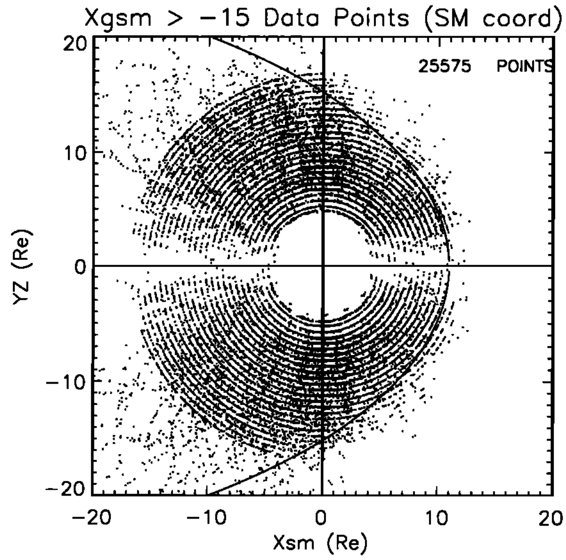

Figure 1a. Data point locations for non-ISEE spacecraft in SM coordinates for $X_{GSM} > -15R_E$. YZ is the distance from the X_{SM} axis. The concentric circle effect is due to averaging IMP data in $0.5R_E$ half integral distances. HEOS spacecraft contribute the data beyond $17R_E$.

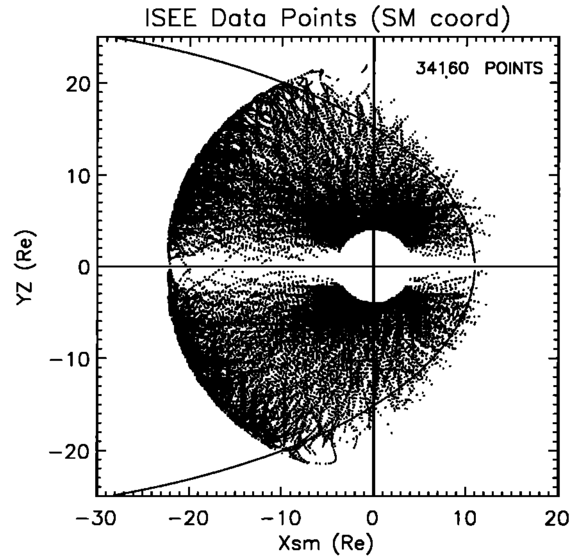

Figure 1c. Data point locations for ISEE 1 and 2 spacecraft in SM coordinates.

of the ordinate is that of Y_{SM}. The solid line represents the average (nonaberrated) magnetopause for $B_z = 0$ and an average pressure of 1.8 nPa as determined by *Roelof and Sibeck* [1993]. If all IMP data are present within a half R_E radial interval the average position falls in the middle of this half-Earth-radii interval leading to the concentric circle effect. Missing data during the averaging interval can lead to a location between the circles, but the majority of these interlying points are from the HEOS spacecraft where a different averaging technique was used (see above). Points outside the concentric circle are also from HEOS.

Figure 1b shows data complementary to Figure 1a only for solar magnetospheric coordinates and for $X_{GSM} < -15R_E$.

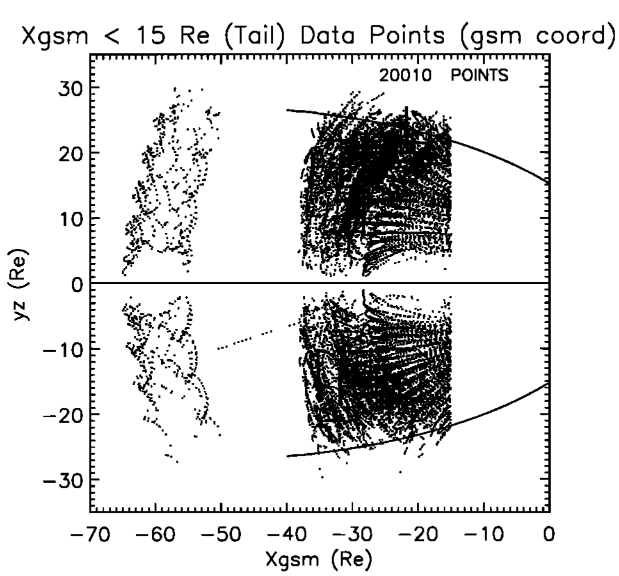

Figure 1b. Data point locations for non-ISEE spacecraft in GSM coordinates for $X_{GSM} < -15R_E$.

Again, ISEE data are not included and the same Roelof/Sibeck magnetopause is indicated by a solid line. IMP 5 data inside an apogee near $29R_E$ can be distinguished, but IMP 4 and 6 data inside apogees near $31R_E$ and $33R_E$ are not so readily distinguished. Explorer 35 contributes all the data near $60R_E$ and its initial pass out to the moon is clear. IMP 7 and 8 contribute the rest of the data beyond $33R_E$. A small number of IMP hourly averages with $X_{GSM} < -15R_E$ and $R < 17R_E$ that would be redundant with the $<17R_E$ averages, have been removed. Note that there will be a lack of IMP points on the dawn and dusk flanks in a small region where $R > 17R_E$ and $X_{GSM} > -15R_E$.

Figure 1c shows ISEE data in the same presentation as Figure 1a and 1b. The concentric circle effect of Figure 1a is missing because of the different averaging method (see above). Note that the 34,160 ISEE data points represent 42.8% of the total data set even though only 4 years of ISEE data are included. This is because (1) ISEE spends a much larger portion of its time inside the magnetosphere compared to the higher apogee IMP and HEOS spacecraft and (2) beyond $15R_E$ in the tail the ISEE averaging technique often produces two values per hour compared to one for the IMP missions.

Figure 2 illustrates data for $X_{GSM} < -15R_E$ projected onto a plane perpendicular to the X_{GSM} axis. The vertical coordinate is the estimated distance from the tail current sheet using the model of *Fairfield* [1980]. Data from the northern and southern hemispheres have been separated according to $B_x > 0$ or $B_x < 0$. ISEE data are shown in the bottom two panels and the remainder of the data in the top two panels. A $20R_E$ circle is shown for reference. Coverage of the tail far from the equatorial current sheet is due largely to the IMP 8 spacecraft. Occasional occurrences of positive (negative) B_x in the southern (northern) hemisphere are probably due largely to solar wind flow out of the ecliptic plane; such effects will be more important at the larger distances and smaller at the closer ISEE distances as appears to be true. Note also that with a primarily northward

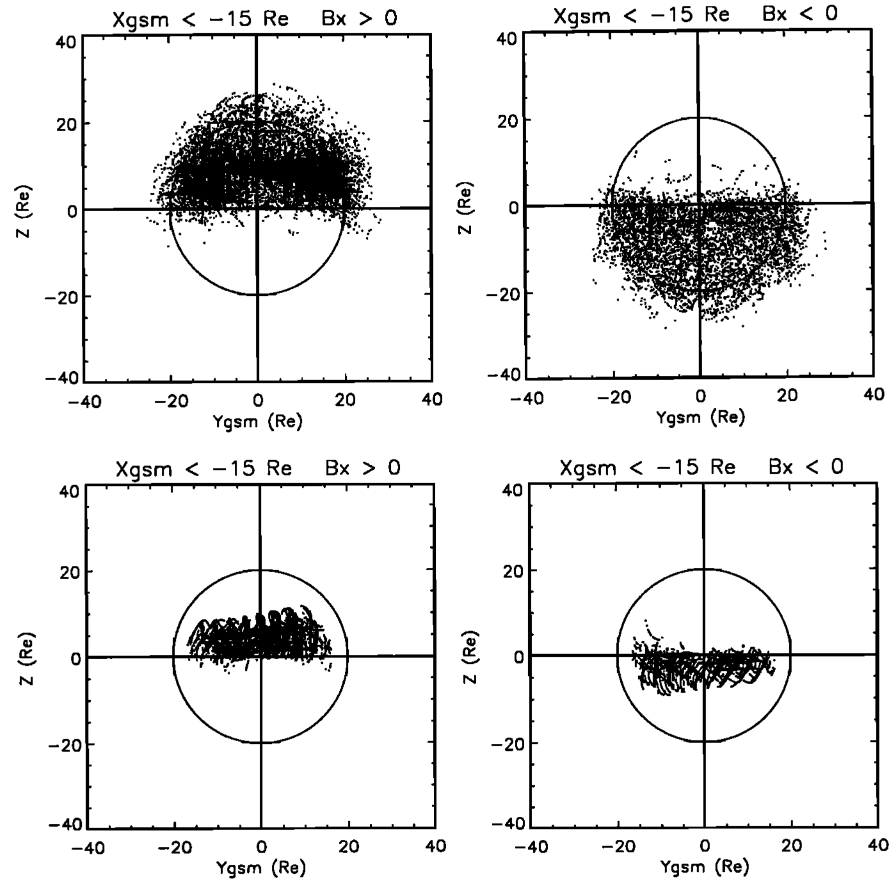

Figure 2. Data point location in the YZ plane for $X_{\mathrm{GSM}} < -15R_E$, where Z' is the estimated distance from the equatorial current sheet. Data have been separated according to the polarity of the B_x component. ISEE 1 and 2 data are shown in the bottom two panels and the other spacecraft in the top panels.

field the positive or negative B_x component may be very small.

The distribution of data with time and by spacecraft is shown in the bottom panel of Figure 3. The solar cycle is indicated by the sunspot number in the top panel and the average annual solar wind kinetic pressure in the second panel [*Fairfield*, 1991]. The number of points contributed by each spacecraft is indicated by the number associated with each label. Spacecraft identification is word number 18 in the

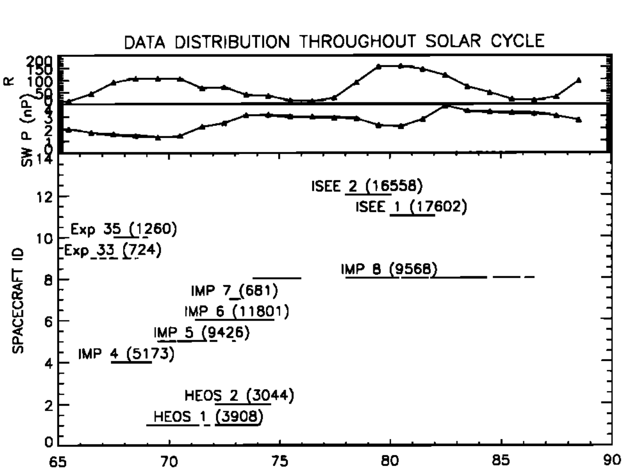

Figure 3. The era of various spacecraft contributions is shown with a horizontal line opposite the appropriate spacecraft identification number. Number associated with the labels indicate the number of data points contributed by each spacecraft. The solar cycle is indicated by the top two traces showing sunspot number R and kinetic solar wind pressure.

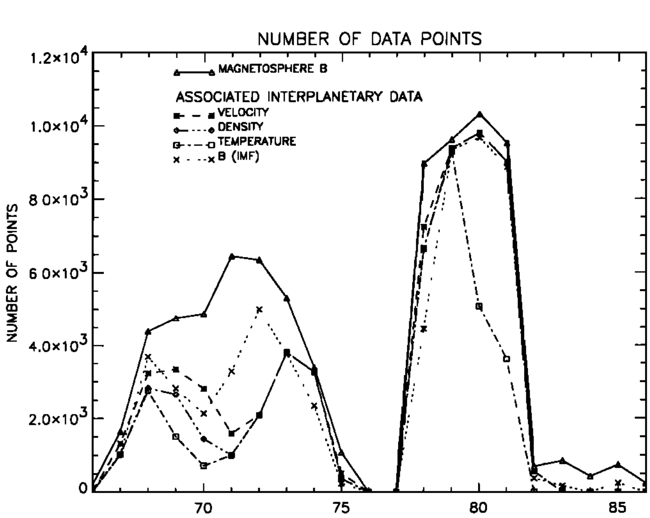

Figure 4. Number of data points/year for the whole data set. Also shown are the number of associated solar wind/IMF values.

Table 2. Format

	Quantity	Format	Description
1	year	I3	two digit year
2	day	I4	day of year (Jan. 1 = day 1)
3	hour	I3	hour of day (0–23)
4	$B_{\min}$	I5	begin time of averaging interval (tenths of minutes)*
5	$D_{\min}$	I5	duration of averaging interval (tenths of minutes)
6	Gl	I5	dipole tilt angle (geomagnetic latitude of Sun) in tenths of degrees (positive in December)
7	X_{GSM}	I7	geocentric solar magnetospheric X position in hundredths of an Earth radii
8	Y_{GSM}	I7	Y position as above
9	Z_{GSM}	I7	Z position as above
10	B	I7	average of individual measured field magnitudes in tenths of nanoteslas
11	$B_{x\mathrm{GSM}}$	I7	average geocentric solar magnetospheric B_x component in tenths of nanoteslas
12	$B_{y\mathrm{GSM}}$	I7	average B_y component as above
13	$B_{z\mathrm{GSM}}$	I7	average B_z component as above
14	$Db_{x\mathrm{GSM}}$	I7	geocentric solar magnetospheric B_x field component minus internal field component in tenths of nanoteslas
15	$Db_{y\mathrm{GSM}}$	I7	B_y field component difference as above
16	$Db_{z\mathrm{GSM}}$	I7	B_z field component difference as above
17	Db	I7	square root of sum of squares of three component standard deviations in tenths of nanoteslas
18	Sat	I3	spacecraft identification number (see Figure 3)
19	Kp	I3	Kp index
20	Dst	I6	Dst index (in nanoteslas)
21	B_{IMF}	I6	average of individual interplanetary field magnitudes in tenths of nanoteslas
22	$B_{x\mathrm{IMF}}$	I6	average of interplanetary B_x in geocentric solar magnetospheric coordinates in tenths of nanoteslas
23	$B_{y\mathrm{IMF}}$	I6	B_y as above
24	$B_{z\mathrm{IMF}}$	I6	B_z as above
25	T	I6	interplanetary proton temperature (in kelvin degrees divided by 1000)
26	N	I5	interplanetary density in tenths of cm^{-3}
27	V	I5	interplanetary velocity, km/s
28	V_{lat}	I5	north-south flow direction in tenths of degree (positive is flow from south)
29	V_{lon}	I5	east-west flow direction in tenths of degree (positive is flow from west of Sun that is, with a duskward component) aberration has been removed
30	AE	I5	AE index (in nanoteslas)
31	AL	I6	AL index (in nanoteslas)

Format (I3, I4, I3, 3I5, 11I7, 2I3, 6I6, 5I5, I6).
*For HEOS the time is the middle of the averaging interval.

record format (see below). Note that the solar wind pressure varying by at least a factor of 2 over the solar cycle can produce different average magnetosphere characteristics at different phases of the cycle.

In Figure 4 we show the number of data points per year and the amount of associated solar wind and IMF data. Note that the best years for solar wind coverage occurred in 1966–1968 and 1972–1974 when many spacecraft were in orbit and in 1978–1982 when ISEE 3 was at the upstream libration point. In 1983, ISEE 3 was moved to the magnetic tail and its solar wind coverage terminated. Note that in 1978–1982 the number of data points per year exceeded the number of hours in a year (8760) largely because ISEE often provided more than one point per hour. Data points beyond 1981 are exclusively IMP 8.

Data Format

The format of the data is shown in Table 2. The four columns in the tables are a word number, an arbitrary abbreviated word name, the integer format, and a description of the word. The data are in fixed point ASCII format, and some quantities have been multiplied by 10 or 100 to preserve decimal accuracy within the integer values. Words 4 and 5 contain the beginning time and duration of the average, except that for HEOS word 4 is the center time of the averaging interval. Note that the average of individual field measurements available as word 10 is different than the square root of the sum of the squares of the components except for HEOS and IMP $< 17R_E$ data where only the latter was available. Words 1–18 contain information related to the magnetic field average while words 18–31 contain solar wind and geomagnetic index information.

All data are given in geocentric solar magnetospheric coordinates. Near the Earth, solar magnetic coordinates are a more appropriate coordinate system and these coordinates are easily obtained by rotating any solar magnetospheric quantities about the Y_{GSM} axis using the transformation

$$X_{SM} = X_{GSM} \cos(gl) - Z_{GSM} \sin(gl)$$

$$Z_{SM} = X_{GSM} \sin(gl) + Z_{GSM} \cos(gl)$$

where gl is the geomagnetic latitude of the Sun or the dipole tilt angle (word 6).

Summary

The large database described here is a significant resource for investigating the distant magnetic field of the Earth as perturbed by the solar wind and IMF. Measurements from 11 different spacecraft provide a total of 79,745 records, each with an average magnetic field vector measured within the magnetosphere somewhere between $4R_E$ and $60R_E$. Each record also has available the measured magnetic field with the Earth's internal field subtracted and also the Kp, Dst, and AE geomagnetic indices and solar wind/IMF values when available (roughly half the time). These parameters will allow sorting the data to study the magnetosphere field configuration under various solar wind and geomagnetic conditions.

The database should be of interest to both students and experienced researchers. Students should be able to use the data to readily demonstrate basic characteristics of the Earth's field. Experienced researchers should be able to look at the data in innovative ways to answer specific questions and extract new knowledge. Magnetic field modelers will want to use words 14–16, which have the internal field subtracted out. Users carrying out statistical investigations of the field will probably use total field components given as words 11–13 in solar magnetospheric coordinates. The data are easily rotated to solar magnetic coordinates using the transformations given above. Rotations to many other coordinate systems can be accomplished using a package of Fortran programs compiled by one of the authors (N.A.T.), which will be made available with the data. The data set is in ASCII format, about 14 megabytes in size and is available from NSSDC. It is planned to make the data set available on CD-ROM sometime in the future.

Acknowledgments. Many individuals are responsible for the contributing the vast amount of data contained in this database. Primary among them are the principal investigators for the magnetic field experiments: N. F. Ness for the IMP experiments (and later R. P. Lepping for IMP 8), P. C. Hedgecock for HEOS, and C. T. Russell for ISEE. Experimenters too numerous to mention contributed plasma and magnetic field data compiled in the OMNI solar wind database by J. H. King and colleagues at NSSDC. The numerous indices included with the data have been compiled by various groups at various times. Programing support of J. A. Jones is also acknowledged. This work was done while one of us (N.A.T.) held an NRC Associateship at NASA GSFC.

The Editor thanks G. L. Siscoe and another referee for their assistance in evaluating this paper.

References

Fairfield, D. H., Bow shock associated waves observed in the far upstream interplanetary medium, *J. Geophys. Res.*, *74*, 3541, 1969.

Fairfield, D. H., Whistler waves observed upstream from collisionless shocks, *J. Geophys. Res.*, *79*, 1368, 1974.

Fairfield, D. H., A statistical determination of the shape and position of the geomagnetic neutral sheet, *J. Geophys. Res.*, *85*, 775, 1980.

Fairfield, D. H., Solar wind control of the size and shape of the magnetosphere, *J. Geomagn. Geoelectr.*, *43*, 117, 1991.

Fairfield, D. H., and N. F. Ness, Imp 5 magnetic-field measurements in the high-latitude outer magnetosphere near the noon meridian, *J. Geophys. Res.*, *77*, 611, 1972.

Hedgecock, P. C., Magnetometer experiments in the European Space Research Organisation's HEOS satellites, *Space Sci. Instrum.*, *1*, 61, 1975.

Hedgecock, P. C., and B. T. Thomas, HEOS observations of the configuration of the magnetosphere, *Geophys. J. R. Astron. Soc.*, *41*, 391, 1975.

King, J. H., Interplanetary medium data book, *NSSDC/WDC-A-R&S 77-04*, p. 1, Natl. Space Sci. Data Cent., Greenbelt, Md., 1977.

Mead, G. D., and D. H. Fairfield, A quantitative magnetospheric model derived from spacecraft magnetometer data, *J. Geophys. Res.*, *80*, 523, 1975.

Ness, N. F., K. W. Behannon, S. C. Cantarano, and C. S. Scearce, Observations of the Earth's magnetic tail and neutral sheet at 510,000 kilometers by Explorer 33, *J. Geophys. Res.*, *72*, 927, 1967a.

Ness, N. F., K. W. Behannon, C. S. Scearce, and S. C. Cantarano, Early results from the magnetic field experiment on lunar Explorer 35, *J. Geophys. Res.*, *72*, 5769, 1967b.

Oglivie, K. W., A. Durney, and T. von Rosenvinge, Descriptions of experimental investigations and instruments for the ISEE spacecraft, *IEEE Trans. Geosci. Electron.*, *GE-16*, 151, 1978.

Peredo, M., D. P. Stern, and N. A. Tsyganenko, Are existing magnetospheric models excessively stretched?, *J. Geophys. Res.*, *98*, 15,343, 1993.

Roelof, E. C., and D. G. Sibeck, Magnetopause shape as a bivariate function of interplanetary magnetic field B_z and solar wind dynamic pressure, *J. Geophys. Res.*, *98*, 21,421, 1993.

Russell, C. T., The ISEE 1 and 2 fluxgage magnetometers, *IEEE Trans. Geosci. Electron.*, *GE-16*, 239, 1978.

Tsyganenko, N. A., A model of the cislunar magnetospheric field, *Ann. Geophys.*, *32*, 1, 1976.

Tsyganenko, N. A., Numerical models of quiet and disturbed geomagnetic field in the cislunar part of the magnetosphere, *Ann. Geophys.*, *37*, 381, 1981.

Tsyganenko, N. A., Global quantitative models of the geomagnetic field in the cislunar magnetosphere for different disturbance levels, *Planet. Space Sci.*, *35*, 1347, 1987.

Tsyganenko, N. A., A magnetospheric magnetic field model with a warped tail current sheet, *Planet. Space Sci.*, *37*, 5, 1989.

Tsyganenko, N. A., and A. V. Usmanov, Determination of the magnetospheric current system parameters and development of experimental geomagnetic field models based on data from IMP and HEOS satellites, *Planet. Space Sci.*, *30*, 985, 1982.

D. H. Fairfield and N. A. Tsyganenko, Laboratory for Extraterrestrial Physics, NASA Goddard Space Flight Center, Code 695, Greenbelt, MD 20771. (e-mail: SPAN.Lepvax::U2DHF;SPAN.Lepvax::Y52NT)

M. V. Malkov, Institute of Informatics and Mathematical Modeling, Apatity 184200, Russia.

A. V. Usmanov, Institute of Physics, University of St. Petersburg, St. Petersburg 198904, Russia.

(Received November 9, 1993; revised January 10, 1994; accepted January 20, 1994.)